Mineralium Deposita (2023) 58:553–568
https://doi.org/10.1007/s00126-022-01141-z

ARTICLE

Controls on Pt/Pd ratios in Bushveld magmas and cumulates: a review complemented by new W isotope data

Wolfgang D. Maier[1] · **Andrea Mundl-Petermeier**[2,3]

Received: 24 December 2021 / Accepted: 22 September 2022 / Published online: 20 October 2022

Abstract

The Bushveld Complex of South Africa is underlain by a fine-grained sill complex which most workers interpret to represent the quenched parent magmas to the intrusion. The sills have unusually high Pt contents (up to ~ 25 ppb) and Pt/Pd ratios (average 1.50) exceeding those in most other mantle magmas globally. Unusually high Pt/Pd is also found in many Bushveld cumulates. Understanding the origin of the high Pt/Pd is important for exploration, in view of the contrasting monetary value of the metals, but also for unravelling the petrogenesis of the intrusion. Here, we review existing platinum-group element (PGE) data and present the first radiogenic W isotope data on a Bushveld rock, to evaluate a range of potential models, including PGE fractionation prior to final magma emplacement and within the Bushveld magma chamber, magma derivation from the sub-continental lithospheric mantle (SCLM), contamination of Bushveld magma with Pt-rich continental crust, and a meteoritic component in the mantle source to the magmas or in the crust with which the magmas interacted. We identify three key processes causing fractionation of metals prior to final magma emplacement and within the Bushveld chamber, namely crystallisation of Pt alloys, partial melting of cumulus sulfides triggered by flux of volatiles followed by sulfide melt percolation, and mobilisation of PGE by percolation of volatiles through the cumulate pile. The currently available W and Ru isotope data are inconsistent with derivation of the Bushveld magmas from mantle or crustal sources containing an enhanced meteoritic component relative to normal post-Hadean mantle.

Keywords Bushveld Complex · Geochemistry · Platinum-group elements · W isotopes · Ru isotopes

Introduction

The Bushveld Complex represents one of the largest magmatic events on Earth, comprising the world's largest mafic–ultramafic layered intrusion as well as vast felsic and mafic lava flows and granite sheets. The Complex hosts the bulk of global platinum-group element (PGE) resources occurring in so-called reefs, i.e., broadly stratiform layers enriched in sulfide and sulfide and platinum-group minerals (PGM) (Smith and Maier 2021). Despite a century of research, the petrogenesis of the reefs remains debated. In part, this is because, for most layered intrusions, the nature of the parent magma(s) is unknown. The Bushveld Complex is an exception in that it is underlain by a suite of fine-grained sills that are considered to represent the parent magmas of the mafic–ultramafic portion of the Complex. Compared to global mafic–ultramafic magmas, the Bushveld magmas have unusually high Pt/Pd ratios averaging 1.5 (Barnes et al. 2010). The specific reasons remain under debate (e.g., von Gruenewaldt and Merkle 1995; Cawthorn et al. 2002; Kinnaird and McDonald 2018). An improved understanding is important for exploration and mining as Pd is currently more than twice as valuable as Pt (~ 2100 USD/oz Pd vs. ~ 900 USD/oz Pt, September 2022). Also, understanding the origin of the variation in Pt/Pd can potentially place added constraints on petrogenetic models for layered intrusions and on the compositional evolution of the Earth's mantle.

Editorial handling: B. Lehmann

✉ Wolfgang D. Maier
maierw@cardiff.ac.uk

[1] School of Earth and Environmental Sciences, Cardiff University, Cardiff CF10 3AT, UK

[2] Department of Lithospheric Research, University of Vienna, 1090 Vienna, Austria

[3] Department of Geology, University of Maryland, College Park, MD 20742, USA

Pt/Pd and Au/Pt ratios in Bushveld magmas

Global komatiites and basalts that crystallised while remaining undersaturated in sulfide melt typically have up to ~20 ppb Pd and Pt (Fig. 1). Pt/Pd ratios cluster around or just below unity, except for relatively evolved lavas many of which tend to have somewhat lower Pt/Pd. The magmas show a subtle trend of increasing Pd and Pt with falling MgO resulting from incompatibility of Pd and Pt into silicate and oxide minerals (Barnes and Ripley 2016). The observed scatter may be due to a combination of mobility of PGE in hydrothermal and low-T fluids, and equilibration with immiscible sulfide melt (notably in some of the relatively evolved samples having < 10 wt.% MgO). In addition, there is a temporal control, in that Archean komatiites tend to have lower PGE than post-Archean lavas (Maier et al. 2009; Puchtel et al. 2020).

The Pd contents of Mg-basaltic to komatiitic Bushveld magmas (so-called Bushveld 1, or B1, magmas; Sharpe 1981) overlap with the Pd-rich samples of the global lavas, but the Bushveld magmas have markedly higher Pt and, somewhat less pronounced, Pt/Pd (Maier and Barnes 2004; Barnes et al. 2010, 2015; Maier et al. 2016) (Fig. 1). Other suites with elevated Pt and Pt/Pd include ~ 2.05 Ga Ti–rich komatiites of the Lapland Greenstone belt (Karasjok and Jeesiovaara, Fiorentini et al. 2011; Puchtel et al. 2020), 2.9 Ga komatiites of Western Australia (Fiorentini et al. 2011), the ~ 260 Ma Emeishan picrites of China (Li et al. 2014), the 120 Ma–recent Kerguelen basalts and picrites (Chazey and Neal 2005), and the ~ 1.27 Ga Coppermine Mg-basalts of northern Canada (Day et al. 2013). For most of these suites, there is no clear trend of PGE content or Pt/Pd against MgO, except for the Jeesiovaara suite analysed by Puchtel et al. (2020) which shows a good negative correlation between Pt and Pd with MgO, and the Bushveld magmas which show a subtle increase in Pt/Pd with falling MgO.

Pt/Pd (and Au/Pt) ratios in Bushveld cumulates

Bushveld cumulates show much more pronounced variation in Pt/Pd than the Bushveld magmas (von Gruenewaldt and Merkle 1995; Cawthorn et al. 2002; Naldrett 2004; Maier and Barnes 2004; Kinnaird 2005; Hutchinson and McDonald 2008; Kinnaird and McDonald 2018; Maier et al. 2021) pointing to the importance of magma chamber processes in controlling at least some of the observed variation. Variation in Pt/Pd occurs at several scales:

1. Regional-scale variation between the western (WBC), eastern (EBC) and northern Bushveld lobes (NBC): This is particularly evident in the well-characterised reef horizons (Naldrett et al. 2009; Fig. 1 in Grobler et al. 2019). For example, the Merensky Reef (MR) of the WBC tends to have Pt/Pd ratios between 2 and 2.5, the MR in the EBC has slightly lower ratios (~ 1.5–2), whereas most of its correlatives in the northern lobe (Platreef, Flatreef and Waterberg deposit) have Pt/Pd between unity and 1.6.
2. Regional variation within individual lobes: For example, in the contact-style mineralisation of the northern Bushveld lobe (Platreef and Flatreef), Pd/Pt is markedly higher in the north than in the south (Maier et al. 2008; Kinnaird and McDonald 2018; McDonald et al. 2017). To some degree, this may be due to the northern prospects representing stratigraphically higher intervals than the southern prospects, as will be discussed in a later section.
3. Large-scale stratigraphic variation: At the base of the WBC layered suite, Pt/Pd is typically relatively low (average of 0.35 in the lower 250 m of the WBC, Fig. 2, Maier et al. 2013). Across the remainder of the Lower Zone (LZ) and much of the Critical Zone (CZ), Pt/Pd shows a progressive increase with height, to peak in the UG1 footwall unit (Pt/Pd > 10) which is characterised by very low Pd values (< 5 ppb) at Pt contents of several tens of parts per billion (Maier et al. 2013). The Main Zone (MZ) and Upper Zone (UZ) have somewhat lower Pt/Pd than the LZ and CZ (Fig. 2). Stratigraphic variation in the northern lobe broadly mirrors that in the WBC, with low Pt/Pd (often < 0.5) at the base and upward increases in Pt/Pd within the Platreef towards values more typical of the CZ of the EBC and WBC (Fig. 3) (Manyeruke et al. 2005; Kinnaird et al. 2005; Ihlenfeld and Keays 2011; Grobler et al. 2019; Maier et al. 2021). The mineralised portions of the MZ have relatively low Pt/Pd, particularly around the Troctolite Marker (Pt/Pd 0.4–0.9, Kennedy 2018) and the Pyroxenite Marker (Maier and Barnes 2010).
4. Stratigraphic variation within individual layers. Examples are the UG1 and UG2 chromitites of the WBC (McLaren and de Villiers 1982; Maier and Barnes 2008) showing Pt/Pd up to > 100 (UG1, Fig. 4), the MG3 chromitite (Pt/Pd from < 1 to ~ 8, increasing upwards) and the MG4a chromitite of the EBC (Pt/Pd < 1 to 14) (Naldrett et al. 2012). The Middling unit at the top of the Flatreef shows a bell-shaped Pt/Pd trend, with an upward increase in Pt/Pd in the lower portion (from ~ 1 to ~ 5) and a decrease (from 5 to ~ 1) through the upper portion (Fig. 5) (Maier et al. 2021).

Analogous to Pt/Pd, ratios of Au/Pt show marked variation in Bushveld cumulates (Figs. 5, 6a). In a broad sense,

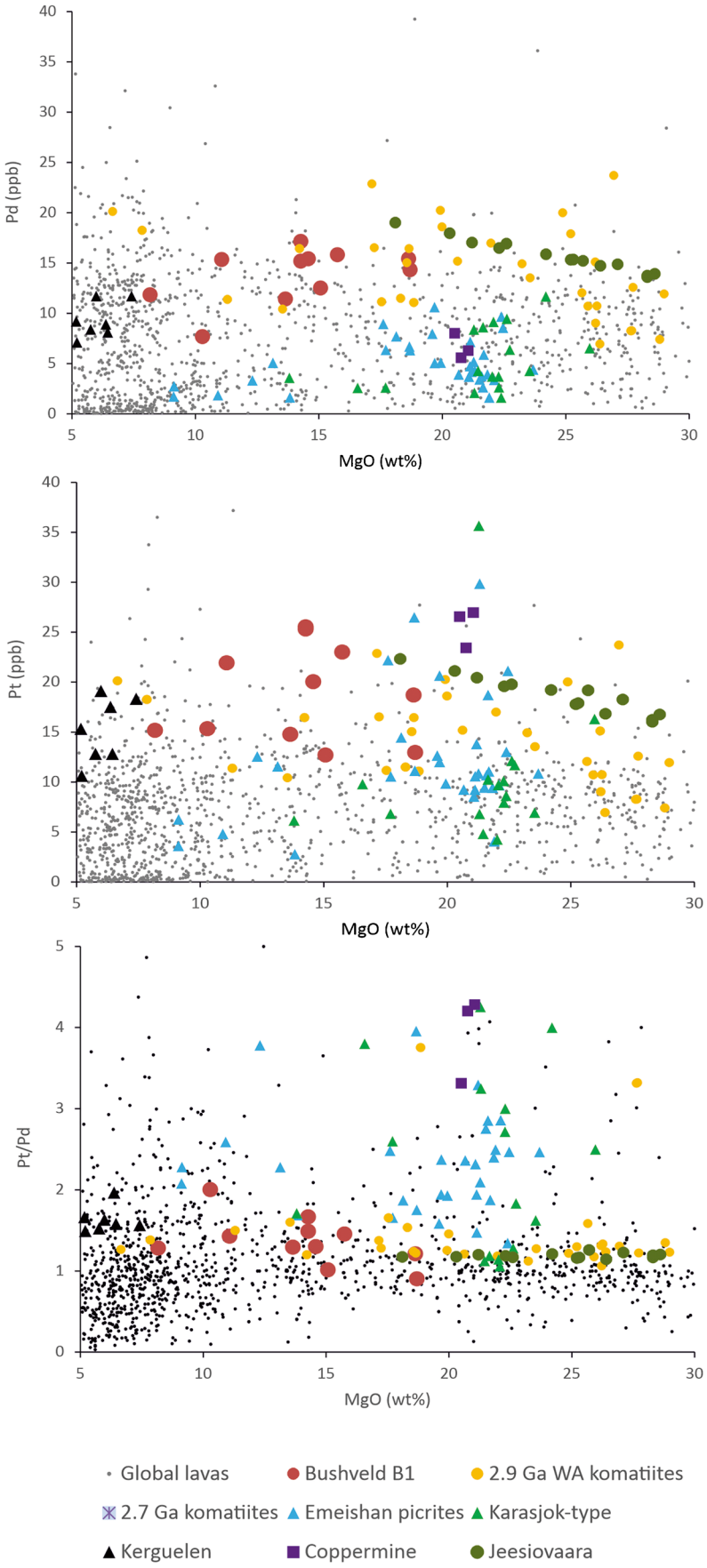

Fig. 1 PGE contents and Pt/Pd ratios in global basalts and komatiites (data from Barnes et al. 2010; Maier et al. 2016; Fiorentini et al. 2011; Puchtel et al. 2020; Li et al. 2014; Chazey and Neal 2005; Day et al. 2013)

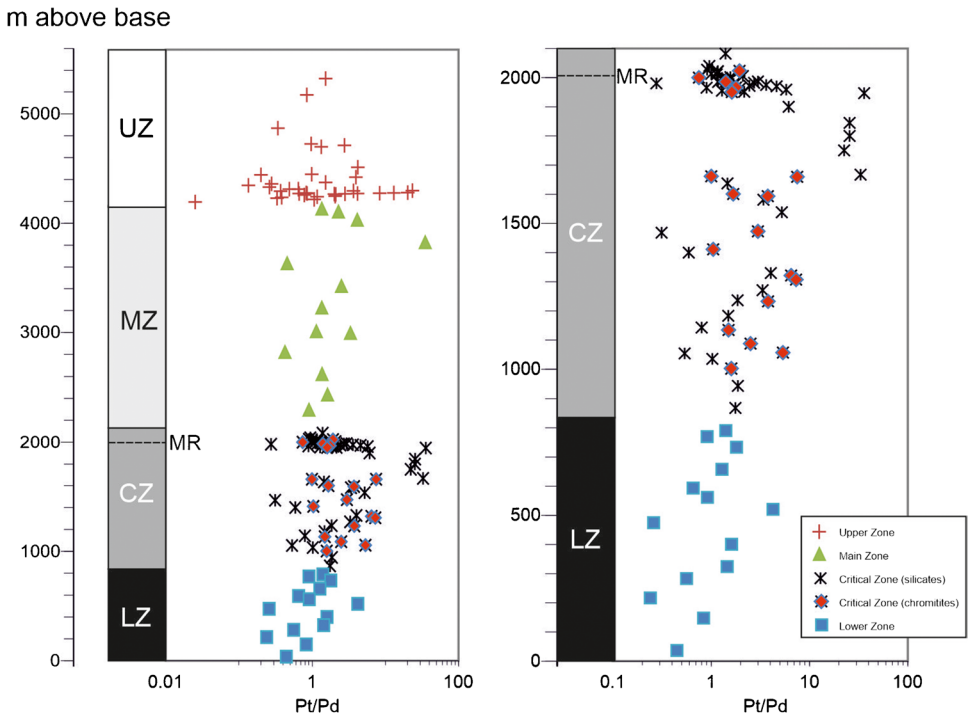

Fig. 2 Variation in Pt/Pd in the layered suite of the Bushveld Complex. Data from Maier et al. (2013)

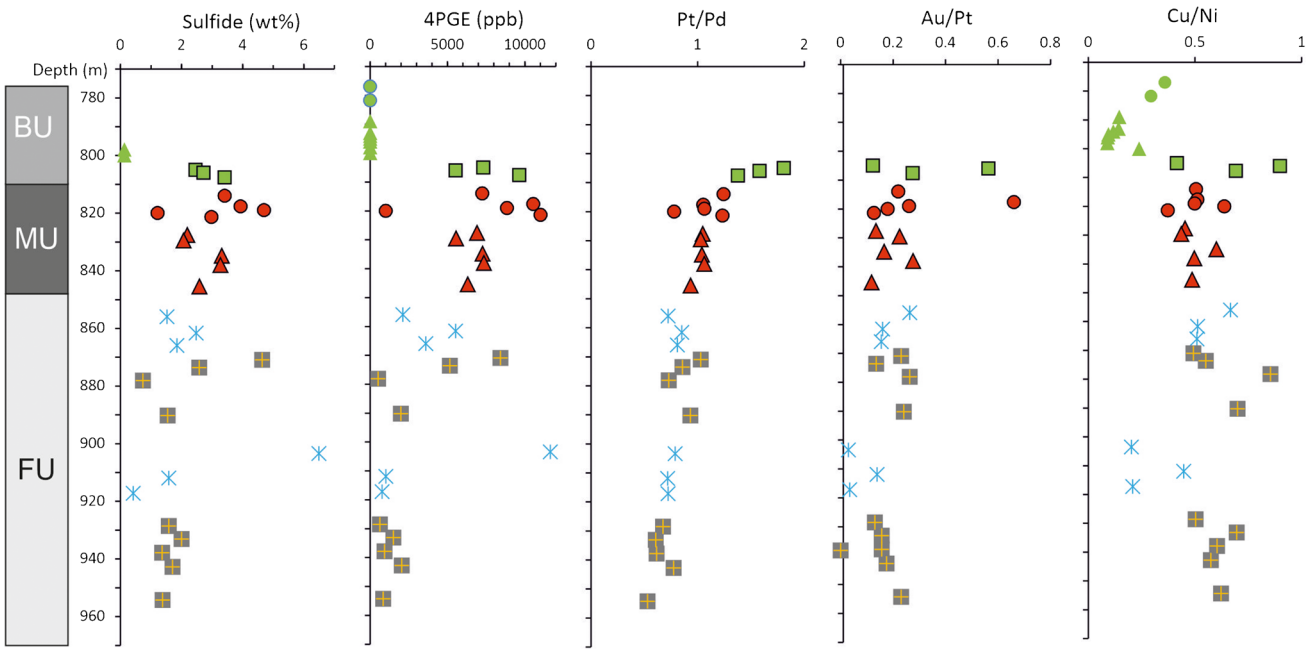

Fig. 3 Compositional variation in the Flatreef, drill core TMT006 (data from Maier et al. 2022). BU, Bastard unit; MU, Merensky unit; FU, Footwall unit. 4PGE = Pt + Pd + Au + Rh

Au/Pt increases with height: Many of the lowest Au/Pt ratios occur in the LZ and CZ, whereas the highest Au/Pt is found in the UZ. In addition, there is pronounced local-scale variation. A particularly marked increase in Au/Pt is seen across the reef interval of the upper CZ (Fig. 6b), and above individual PGE reefs (e.g. UG1 and UG1, Merensky and Bastard Reefs, Maier and Barnes 2008; Maier et al. 2021).

Smaller-scale variation can be studied, e.g., in the Flatreef of the NBC where continuous assays are available over the reef intervals. Au/Pt ratios show little systematic stratigraphic

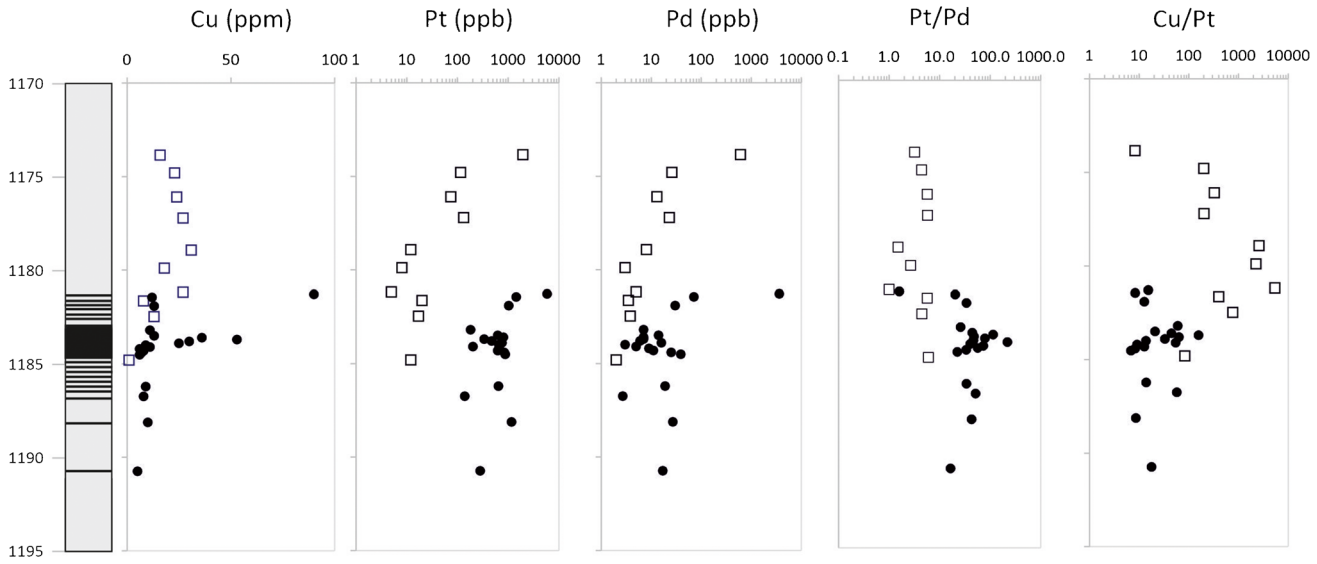

Fig. 4 Compositional variation in the UG1 chromitite, Impala platinum mine (from Maier and Barnes 2008)

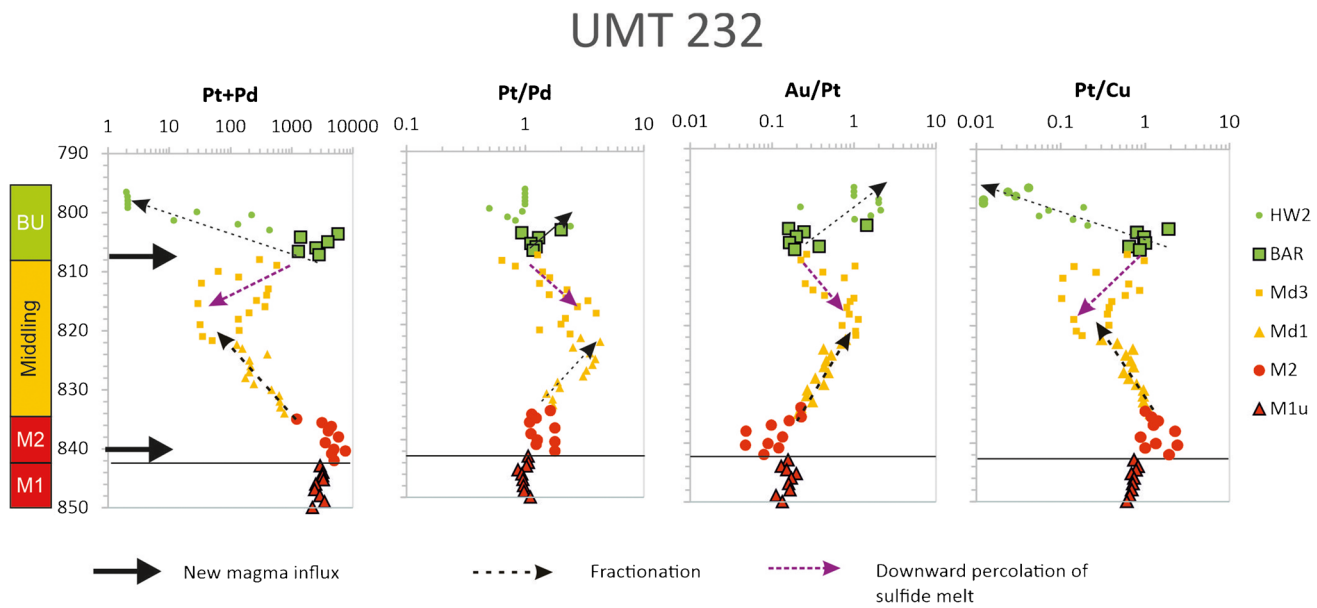

Fig. 5 Variation in PGE, Pt/Pd, Au/Pt and Pt/Cu in uppermost Flatreef, northern Bushveld lobe (data from Maier et al. 2021)

variation throughout much of the Flatreef (Maier et al. 2021, 2022) except for a marked increase above the Merensky Reef, i.e. in the Middling and Bastard units (Fig. 5), correlating with an analogous increase in Pt/Pd, and a decrease in Pt + Pd and Pt/Cu. In the upper portion of the Middling unit, the trend of increasing Au/Pt and Pt/Pd, and decreasing Pt/Cu and Pt + Pd, is reversed, resulting in a bell-shaped pattern for the entire interval.

High Au/Pt ratios, at variable Pt/Pd, are also characteristic of many of the MZ-associated mineralisations in the northern lobe, e.g., in the Waterberg T zone (Kinnaird et al. 2017), the basal mineralisation at Nonnenwerth/Aurora (Manyeruke 2007; Maier et al 2008; McDonald et al. 2017) and the Pyroxenite Marker mineralisation at Moorddrift (Maier and Barnes 2010; Holwell et al. 2013).

Tungsten isotope analysis

Tungsten concentrations were measured by isotope dilution using the Element 2 single-collector ICP-MS at the University of Maryland, USA. Tungsten isotopic compositions were determined using a four-step ion exchange chromatography method described in Peters et al. (2019). Isotope compositions

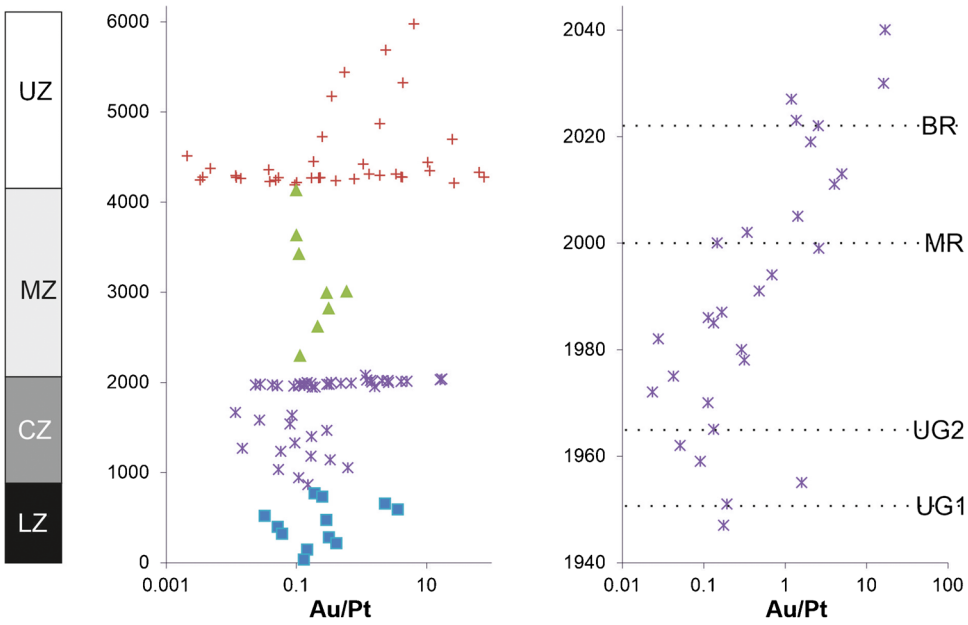

Fig. 6 Au/Pt across the Bushveld Complex at Union Section (data from Maier et al. 2013)

were measured by thermal ionisation mass spectrometry in negative ionisation mode using a Thermo Fisher Triton at the University of Maryland following the method of Archer et al. (2017). Radiogenic W isotope compositions are presented using the μ-notation which defines the parts-per-million deviation of a sample's ^{182} W/^{184} W ratio from that of repeated measurements of a laboratory solution standard (*Alfa Aesar*) that is representative of bulk silicate Earth composition ($\mu^{182}W = 0$; e.g. Walker 2016).

Tungsten isotope compositions of sample 774.11, representing the komatiitic chilled margin of the LZ at Union section, exposed in drill core NG2 (Maier et al. 2016) are presented in Table 1 and show no deviations in $\mu^{182}W$ normalised to ^{183} W/^{186} W (N6/3) and $\mu^{183}W$ normalised to ^{184} W/^{186} W (N6/4), respectively, from the average of seven laboratory standard analyses (2SD = 4.5 and 8.0, respectively).

Discussion

Origin of high PGE and Pt/Pd in Bushveld parent magmas

Melting of sub-continental lithospheric mantle (SCLM)

Based on the relatively high Pt/Pd in Bushveld magmas (Pt/Pd average ~ 1.5) and Kaapvaal SCLM (average Pt/Pd ~ 2; Maier et al. 2012 and references therein) together with unusually high contents of many incompatible trace elements, pronounced negative Nb, Ta and Ti anomalies in multi-element variation diagrams, relatively high SiO_2 contents (up to 55 wt.% SiO_2 at MgO 12–14 wt.%), the predominance of orthopyroxene over clinopyroxene, and elevated Sr and low Nd isotope compositions, Maier and Barnes (2004) suggested that the Bushveld magmas represent partial melts of the SCLM. Richardson and Shirey (2008) and Mungall and Brenan (2014) concurred with this model, based on Os isotopes in diamond inclusions, experimental data and thermodynamic modelling. However, Maier et al. (2016) used MELTS modelling to show that partial melts of fertile Kaapvaal SCLM are Si depleted and K enriched relative to Bushveld komatiite as intersected in a chilled margin at the base of the Complex. The authors concluded that the Bushveld parent magmas likely represent asthenospheric partial melts modified by contamination with the continental crust (see discussion below). A small SCLM component remains a possibility, being that the Bushveld magmas likely ascended through the thick SCLM keel underlying the Kaapvaal craton. However, in view of the generally relatively low PGE contents of the Kaapvaal SCLM (average of ~ 4 ppb Pt, 2 ppb Pd, maximum of 18 ppb Pt and 10 ppb Pd; Maier et al. 2012), this would likely not have significantly influenced the PGE budget of the magmas, unless there are very PGE-rich segments in the SCLM that remain undiscovered or have been consumed by the melting.

Table 1 Tungsten isotope composition, W and Th concentrations

Sample	$\mu^{182}W_{N3/6}$	2SE	2SD (*n*)	$\mu^{183}W_{N4/6}$	2SE	2SD (*n*)	W (ppm)	Th (ppm)	W/Th
774.11	2.1	3.6	4.7 (7)	4.4	4.1	8.0 (7)	0.772	0.35	2.2

2SE represents the uncertainty of the run. 2SD represents the external precision of repeated measurements of laboratory standards ($n = 7$) of the session

Assimilation of Pt-rich crustal sediments and cumulates

Apart from SCLM derivation, the main alternative model to explain the enriched nature of the Bushveld Complex has been crustal contamination of asthenospheric magma (Kruger and Marsh 1982; McCandless and Ruiz 1991; Maier et al. 2000; Harris et al. 2005). However, the available data on Kaapvaal sedimentary rocks provide no strong support for the idea that crustal sedimentary contamination added significant Pt to the magmas. Stephenson (2018) found Pt/Pd mostly above unity in the floor rocks to the northern lobe, but at mostly low PGE contents (< 10 ppb Pt and Pd), consistent with previous studies on Kaapvaal sediments (Siebert et al. 2005; Nwaila and Frimmel 2019; Wille et al. 2007).

Pd mobility through alteration

Based on empirical (Barnes and Liu 2012; Holwell et al. 2017) and experimental (Hanley 2005; Sullivan et al. 2021) evidence, it is normally argued that at typically magmatic conditions (sulfide present, fO_2 near QFM and near neutral pH), Pd is more mobile in fluids than Pt. One could thus argue that the Bushveld fine-grained floor sills were affected by alteration from percolating late-magmatic or metamorphic fluids resulting in loss of Pd and relatively high Pt/Pd. This model was proposed to explain the high Pt/Pd of the Kerguelen lavas (Fig. 1) (Chazey and Neal 2005). However, in the case of the Bushveld magmas, the model is rejected as the fine-grained floor sills have mantle like S/Se and show no petrographic evidence of significant alteration.

The sills are not parental to the cumulates but instead represent residual liquids expelled from the cumulates

Sharpe and Hulbert (1985) and Yao et al. (2021) argued that the medium-grained pyroxenitic and peridotitic floor sills (B1u) represent ejections of crystal mushes from the LZ, perhaps triggered by tectonic adjustment of the Bushveld magma chamber. This would imply that the sills are not representative of the parent magmas to the Bushveld LZ and LCZ, but instead represent residual melts from the cumulates. A similar model was proposed by Helz (1987) for the Stillwater floor dykes. Thus, liquid ejection from the magma chamber was clearly part of the thinking at the time. However, this model is not consistent with PGE systematics. Much of the LZ contains elevated PGE (Maier et al. 2013) suggesting either that the rocks crystallised from sulfide-saturated magma, that sulfide melt percolated downwards from above or that PGE were introduced by reactive flow of volatiles from the interior of the intrusion. If the sills were ejected residual liquids from the cumulates, they should mirror the elevated and heterogeneous PGE contents of the cumulates, yet the sills are undersaturated in sulfide melt and have fairly homogeneous PGE patterns (Barnes et al. 2010). One could argue that the sills lost Pd (and S) during metamorphism, but the S/Se of the sills is mantle-like and not suggestive of significant element mobility, unless S and Se were removed together at high T (Wulf et al. 1995). Another argument against the Yao et al. model is that the Dullstrom lavas which cannot represent residual liquids expelled from the cumulates also have the characteristic high Pt/Pd of the B1–B3 Bushveld basalts (albeit at somewhat lower total PGE contents; unpublished data of Hannah Hughes).

Melting of PGE-rich mantle domains

The PGE contents of the Earth's modern mantle are largely the result of processes occurring during the Hadean and Archean eras: (1) The vast bulk of the Earth accreted ~ 4.5 Ga ago from impactors that remain incompletely known and appear not to be represented in our meteorite collections (Fischer Goedde et al. 2020). (2) Next, the Earth's core formed via segregation of Fe–Ni alloy (and some sulfide) ~ 30 m.y. after Earth's initial accretion (Kleine et al. 2002). The segregation of the core resulted in efficient scavenging of the highly siderophile and chalcophile PGE and Au from the Earth's mantle (Stevenson 1981). (3) The mantle was refertilised with PGE and Au by late accretion (Late Veneer) of impactors from ~ 4.5 to ~ 3.8 Ga, including a final surge (the late heavy bombardment, LHB) at ca. 3.8 Ga. Based on PGE systematics, it is estimated that the LV added ~ 0.5% to the mass of the Earth (Walker 2009). The most important impactors were likely carbonaceous chondrites (Fischer Goedde et al. 2020) which tend to have ~ 0.9–1.2 ppm Pt and 0.6–0.8 ppm Pd, i.e., they have Pt/Pd significantly above unity (Fischer Goedde et al. 2010; Horan et al. 2003; Day et al. 2016). Other potential impactors include iron meteorites representing the cores of asteroids and planets. These have markedly higher Pt (up to > 30 ppm) and Pt/Pd (~ 3–20) (Day et al. 2016). The rate of mixing and equilibration of the Late Veneer into the convecting mantle remains debated: Maier et al. (2009) suggested a timespan of ca. 1.5 Ga (i.e. until ~ 3 Ga) based on PGE contents in komatiites, whereas Puchtel et al. (2020) suggested that portions of the mantle remained poorly equilibrated with LV until ~ 2 Ga, based on W and Pt isotopes as well as PGE systematics in komatiites of the Lapland Greenstone belt. Heterogeneous inmixing of late veneer is consistent with models of modern mantle dynamics; for example, Barry et al. (2017) showed that whole-mantle convection may preserve long-term global patterns of upper-mantle geochemistry. Based on these data, one could hypothesise that the Pt-rich Bushveld magmas formed from a mantle that was relatively enriched in late veneer.

The idea is potentially testable using the short-lived radiogenic ^{182}Hf–^{182} W isotope system, where Hf is lithophile and W a moderately siderophile element. This system is only alive during the first ~ 60 Ma into Earth's history (Vockenhuber et al. 2004). Hence, variations in Earth's rock record must be attributed to Hadean processes, such as metallic core segregation and/or silicate differentiation. μ^{182}W in terrestrial reservoirs shows considerable variation, with Earth's core being less radiogenic ($\mu^{182}W = -220$ ppm) than bulk Earth ($\mu^{182}W = -200$ ppm), bulk silicate Earth and modern upper mantle (μ^{182} W = 0 ppm) (Fig. 7A) (Walker 2016 and references therein). The assumption is that during Hadean core formation, most of the Earth's Hf remained in the mantle due to the incompatibility of Hf with regard to Fe–Ni alloy. Thus, little ^{182} W could be produced via radiogenic decay of ^{182}Hf in the core, resulting in relatively low ^{182} W/^{184} W. In contrast, the Hadean mantle became enriched in ^{182} W, the daughter isotope of ^{182}Hf. The relative enrichment of the Hadean (and early Archean) mantle in ^{182} W is reflected in high μ^{182}W of early-mid Archean lavas and cumulates (Tusch et al. 2021a, b). It is assumed that prior to late accretion, the early Earth's mantle was about 25–30 ppm more radiogenic in terms of μ^{182}W than it is now. Late accretion of largely chondritic material (μ^{182}W

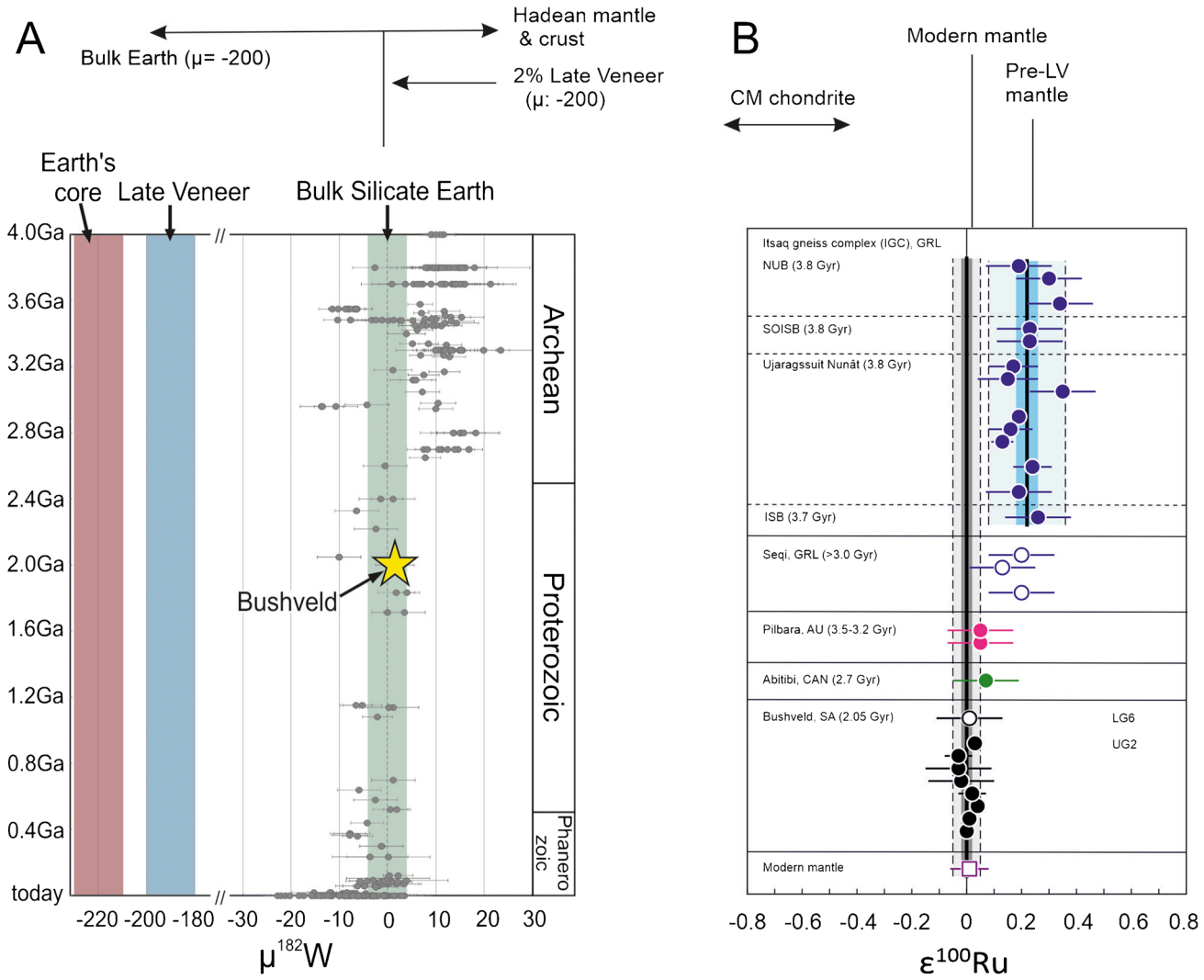

Fig. 7 W and Ru isotope data of Bushveld compared to global data. (**A**) Tungsten isotope compositions of terrestrial rock samples (from Willbold et al. 2011, 2015; Touboul et al. 2012, 2014; Mundl et al. 2017, 2018; Mundl-Petermeier et al. 2019, 2020; Rizo et al. 2016, 2019; Mei et al. 2020; Tusch et al. 2019, 2021a, b; Reimink et al. 2018, 2020; Puchtel et al. 2016a,b, 2018, 2020; Kruijer and Kleine 2018; Liu et al. 2016; Dale et al. 2017; Archer et al. 2019; Tappe et al. 2020; Nakanishi et al. 2021; Peters et al. 2021). The yellow star shows Bushveld sample 774.11 from this study. The green bar represents μ^{182} W of bulk silicate earth (0 ± 4.5). The blue and red bars show the proposed compositions for a chondritic late veneer component and Earth's core, respectively (from Touboul et al. 2012). (**B**) Figure modified from Fischer-Goedde et al. (2020)

= ~ 180-200) shifted the tungsten isotopic composition of the mantle to the present value of $\mu^{182}W = 0$. The near-zero $\mu^{182}W$ of post-Archean rocks is thus normally interpreted to result from partial melting of mantle refertilised with LV, whereas the higher $\mu^{182}W$ of the older rocks is interpreted to reflect melting of mantle that had failed to equilibrate with LV. One could thus suggest that portions of the mantle containing a relatively high component of LV have lower $\mu^{182}W$ than bulk silicate Earth ($\mu^{182}W = 0$).

To test whether this model could apply to Bushveld, we analysed the komatiitic chilled margin of the Complex (sample 774.11 of the NG2 drill core at Union section; Maier et al. 2016). This yielded $\mu^{182}W + 2.1 \pm 3.6$ (Table 1), suggesting that the sample comes from normal mantle without LV-enriched or -depleted domains. However, field relationships (e.g. the presence of several quartzite xenoliths in the basal interval) and trace element systematics suggest that the sample has undergone some pre-emplacement and syn-emplacement contamination (Maier et al. 2016). The relatively high W/Th ratio of ~1 - 2.2 suggests that the rock could have been affected by percolation of a W-rich volatile phase. The contaminants could have had "normal" $\mu^{182}W$, thereby potentially altering an originally negative $\mu^{182}W$ signature. Another possibility is that the Bushveld source could have contained a component of unequilibrated iron meteorite. Iron meteorites have even lower $\mu^{182}W$ and higher W concentrations than chondritic material. Hence, if the source was affected by an iron meteorite, then the 'original,' as in pre-contaminated, W signature could have been even more negative.

Another tool that could be used to evaluate the presence of mantle domains in the Bushveld source is nucleosynthetic Ru isotopes (Fig. 7B). Fischer Goedde et al. (2020) have established that the early (pre-LV) Earth had positive $\varepsilon^{100}Ru$. The authors applied mass balance to argue that the late veneer must have had negative $\varepsilon^{100}Ru$ and that efficient mixing of this LV with the Hadean mantle resulted in $\varepsilon^{100}Ru = 0$ (i.e. the value of bulk silicate Earth). Magmas derived from hypothetical LV-enriched mantle domains should thus have negative $\varepsilon^{100}Ru$. The first Ru isotope data on Bushveld (on UG2 and LG6 chromitite; Fischer-Goedde et al. 2020) overlap with the modern mantle estimate, similar to our W isotope data.

We conclude that the currently available data provide no support for the idea that the Bushveld was sourced from LV-enriched mantle. However, the amount of data generated so far is relatively small and more work is clearly needed.

Contamination of mantle magma by a crustal meteoritic component (e.g. impact structures)

Based on presumed coevality between the Bushveld Complex and the Vredefort impact structure, Dietz (1963), Hamilton (1970) and Rhodes (1975) suggested that the Bushveld formed via a meteorite impact. It is now known that Vredefort is ~ 33 Ma younger than the Bushveld (Kamo et al. 1996). No evidence of shatter cones or high-P minerals has been found in the floor rocks of the Bushveld Complex (French and Hargraves 1971). However, it is conceivable that the Bushveld intrusion could have cannibalised much of the structural and mineralogical evidence of a major impact (Fig. 8). As demonstrated above, W and Ru isotope data as well as PGE contents of Bushveld ultramafic cumulates and magmas provide no clear evidence of a meteoritic component, possibly because the composition of ultramafic rocks shows some overlap with mantle rocks. A possible additional test could be to look for the compositional signature of an asteroid in the felsic lavas and granites which occur on top of the Rustenburg Layered Suite (RLS) and which must have ascended through any putative impact melt sheet at depth. As yet, no PGE data are available for the granites or rhyolites, but we note that the Dullstroom andesites have elevated Pt/Pd analogous to the RLS (unpublished data of Hughes). We conclude that there is currently no evidence for interaction of the lavas with a crustal meteoritic component, but due to paucity of data, this cannot be ruled out at present.

Origin of Pt/Pd variation in Bushveld cumulates

Bushveld cumulates show enormous variation in Pt/Pd (and Au/Pt), in stark contrast to the fine-grained sills with their relatively homogeneous PGE contents and Pt/Pd (and Au/Pt). This suggests that, compared to the sills, in the main Bushveld magma chamber, several additional processes operated that fractionated the PGE and Au from each other. Four main models are considered in the following. All likely applied at some stage during the solidification of the complex.

Primary magmatic fractionation of Pt, Pd and Au due to variable compatibility into crystallising sulfide melt and oxide crystals

The variation in Pt/Pd in the Bushveld cumulates could be the result of differences in $D_{\text{sulfide melt/silicate melt}}$ for Pt and Pd during crystallisation. As noted previously, some of the available experimental data show a somewhat higher compatibility of Pd than Pt with regard to sulfide melt (see summary in Barnes and Ripley 2016). One could propose that this is responsible for the relatively low Pt/Pd at the base of many layered intrusions, including Duluth (Barnes et al. 1997), Muskox (Barnes and Francis 1995) and intrusions in the Cape Smith belt (Barnes et al. 1992). For example, in the Cape Smith intrusions, sulfides have Pd/Pt ratios from 1 to 4, whereas the basaltic komatiites interpreted to represent the parent magmas have Pt/Pd at approximately unity. In the Bushveld magmatic province, one of the most notable examples of relatively low Pt/Pd at the base of an intrusion is the Uitkomst satellite intrusion which contains economically

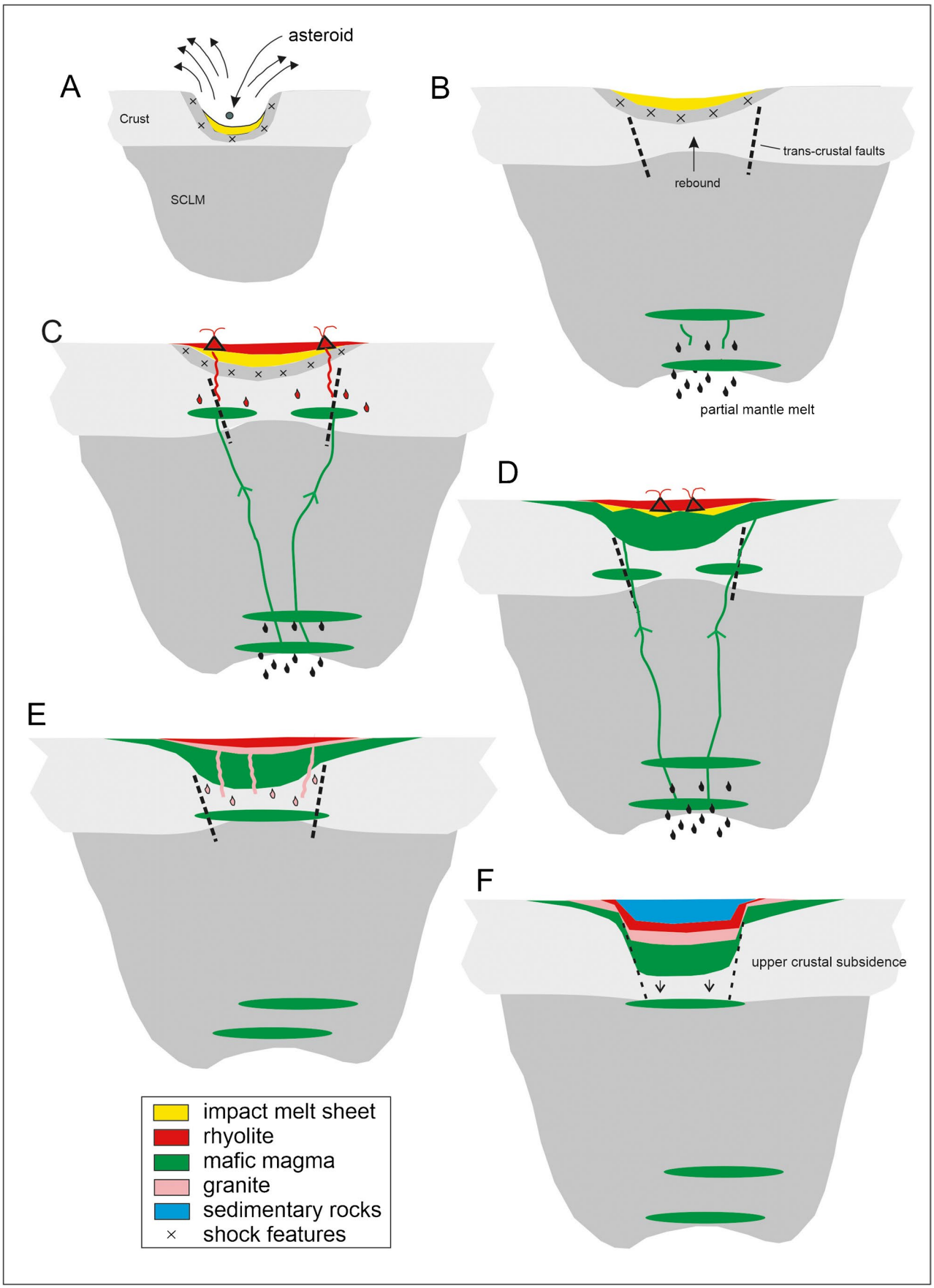
A
asteroid
Crust
SCLM
B
trans-crustal faults
rebound
partial mantle melt
C
D
E
F
upper crustal subsidence
impact melt sheet
rhyolite
mafic magma
granite
sedimentary rocks
shock features

◂**Fig. 8** Sketch model to explain possible formation of Bushveld Complex by asteroid impact. (**A**) Impact of asteroid excavating several kilometres of crust and resulting in shock features, followed by formation of crustal melt sheet. (**B**) Lithospheric rebound results in transcrustal faults and partial melting of uppermost convecting mantle, followed by ascent of mantle melt into lithosphere. (**C**) Mantle melts ascend into crust along transcrustal faults forming layered intrusions. Partial melting of crust by heat of mafic magma generates rhyolitic magma that erupts to form Rooiberg Group deposited on top of crustal melt sheet. (**D**) Continued ascent of mantle melt ponding below, and largely assimilating, crustal melt sheet and rhyolite, forming RLS. Shock features are assimilated. (**E**) Ongoing partial melting of crust by Bushveld magmas generates granite magma which is emplaced below Rooiberg Group. Remnants of the impact melt sheet may be assimilated by granite. (**F**) Bushveld Complex undergoes crustal subsidence contemporaneous with sedimentation of Waterberg and Karoo Supergroups. Any portions of the impact melt sheet, or possible asteroidal fragments, that may not have been assimilated by mafic and felsic Bushveld magmas are buried at depth

important sulfide mineralisation in its basal portion having Pt/Pd around 0.5, whereas (uneconomic) reef-style sulfides in the upper portion of the intrusion have Pt/Pd ~ 1.2 (Maier et al. 2022).

Within the Bushveld Complex itself, Maier et al. (2022) have proposed that differences in D between Pt and Pd can explain intra-layer variation in Pt/Pd occurring on a scale of meters to tens of meters (e.g. Figures 2–5). In the uppermost portion of the Flatreef (MU and BU), trends in metal contents and metal ratios resemble those of classical offset patterns described from, e.g., Munni Munni (Barnes 1993) or Great Dyke (Wilson 2001). Thus, Rh tenors in the upper portion of the main mineralised interval (M2 and BAR) are 67–76% of those in the lower portion (M1), Pd tenors in the upper portion are 79–87% of M1, Cu tenors are 90–92% of M1, Pt tenors are 107–120% of M1 and Au tenors are 149–202% of M1. These data could suggest that the offset patterns result at least partly from sulfide melt fractionation, with $D_{Pd} > D_{Pt} > D_{Au}$, consistent with some of the published data (Barnes and Ripley 2016). Also, Au/Pt shows a marked increase above the UG1, UG2, Merensky and Bastard Reefs (Fig. 6) (Barnes and Maier 2002; Maier and Barnes 2008) and Au/Pt is markedly elevated in many of the reefs in the Northern Lobe which occur at stratigraphically elevated levels, e.g., the Waterberg T zone (Kinnaird et al. 2017), the Platreef at Nonnenwerth/Aurora (Manyeruke 2007; Maier et al. 2008; McDonald et al. 2017) and the Pyroxenite Marker mineralisation at Moordrift (Maier and Barnes 2010).

However, modelling suggests that variation in $D_{\text{sulfide melt-silicate melt}}$ is unlikely to be the only reason for the observed trends. At the relatively low R factors (mass ratio of silicate to sulfide melt; Campbell and Naldrett 1979) applicable to the basal mineralisation in the Flatreef (~ 1000; Maier et al. 2022), and assuming that B1 magma has Pt = 19 ppb and Pd = 14 ppb (Barnes et al. 2010), and $D_{\text{sulfide melt/silicate melt}}$ is 10,000–1,000,000 (Barnes and Ripley 2016), modelled Pt tenors of sulfide are higher than Pd tenors because the tenors are more sensitive to the difference in PGE content (i.e. the higher Pt than Pd content) of the magmas than to potential differences in D. For example, to explain the observed, relatively high Pd/Pt of up to 2 in the basal Flatreef mineralisation, a relatively low D of around 2000 for Pt is required, but none of the experiments give such low values. Similarly, we cannot model the high Pt/Pd (~ 5) in the Middling unit (Fig. 5) by applying realistic D values, nor can we explain the extremely high Pt/Pd in some chromitites (e.g. at the base of the Merensky Reef; Barnes and Maier 2002).

With regard to PGE fractionation triggered by oxide crystallisation, Finnigan et al. (2008) proposed that the commonly observed spatial association of laurite with chromite may be due to localised reduction of the magma within micrometric melt domains surrounding the growing chromite crystals in response to scavenging of Fe^{3+} by the crystallising chromite. Chromitites tend to be highly enriched in Pt and have high Pt/Pd (Barnes and Maier 2002, Fig. 4), suggesting that local-scale magma reduction during chromite crystallisation could also trigger formation of Pt alloys.

Pt and Pd fractionation caused by percolation of sulfide melt through cumulate mushes

Magmatic sulfide melt is relatively dense (4.0 and 4.5 g cm^3; Mungall and Su 2005) and solidifies at relatively low T (~ 700 °C; Helmy et al. 2021). Thus, it could potentially percolate through partially solidified mafic–ultramafic cumulates as long as the silicate grain size is relatively large and sulfide droplets are either smaller than the nodes, or large enough to have sufficient gravimetric power (Chung and Mungall 2009). Percolation of sulfide melt through Bushveld cumulates has been proposed previously for the Merensky Reef (Leeb-du Toit 1986; Godel et al. 2006; Smith et al. 2020) and in the Flatreef (Maier et al. 2022) where downward decreasing PGE and sulfide contents are accompanied by subdued PGE fractionation. In addition, the peculiar bell-shaped PGE and Pt/Pd distribution in the barren Middling unit, interleaved between BAR and M2 (Fig. 5), was interpreted to result from a combination of PGE fractionation (from relatively low Pt/Pd in the basal M2 reef to high Pt/Pd in the PGE depleted rocks above M2) and downward percolation of BAR sulfides into the upper portion of the Middling.

As has been explained above, fractionation of primary magmatic sulfide melt is unlikely to cause Pt–Pd fractionation on the scale observed. However, if solid sulfides undergo partial melting, e.g., in response to volatile fluxing, Pt and Pd have been shown to fractionate (Peregoedova et al. 2004), by generating a Pd–Cu–Ni-rich sulfide melt and refractory Pt-rich PGM. In the context of the Flatreef, we

propose that volatiles ascending from the metamorphosed floor and/or the cooling cumulates pile caused desulfidation and melting of sulfides in the upper Flatreef (M1, M2 and BAR) resulting in downward percolation of a Pd–Cu–Ni sulfide melt contributing to progressively lower Pt/Pd of the Flatreef with depth (Fig. 3), at broadly constant Cu/Ni. The model could also explain the presence of Pd-rich sulfides in calcsilicate interlayers within the lower Flatreef and the sedimentary floor rocks (unpublished data of authors) and, via restitic Pt-rich sulfides and PGM, the high Pt/Pd (up to 5) in the Middling unit (Fig. 5).

Mobilisation of PGE (particularly Pd and potentially Au) in a volatile phase

Experimental data indicate that under certain conditions (acidic pH, high salinity, no sulfide in rock), Pt and Pd can be mobile in magmatic and hydrothermal volatiles, and Pd tends to be more mobile than Pt (Peregoedova et al. 2006; Hanley et al. 2005; Boudreau and McCallum 1992; Boudreau 2019; Sullivan et al. 2021). A volatile phase could be generated during advanced crystallisation of the cumulates, or via metamorphism of the floor rocks. In the Bushveld, there is empirical evidence for both Pt and Pd mobility, e.g., in the form of Pt-enriched hydrothermal veins at Waterberg (McDonald et al. 1999) and extremely Pd-depleted UG1 chromitite intersections (Maier and Barnes 2008). Volatiles could also have played a role in causing the unusually high Pt/Pd of the Merensky Reef Cr stringers; Naldrett and Lehmann (1988) and Li et al. (2005) have suggested that this is due to reaction of sulfide with chromite leading to desulfidation and associated mobility of Pd whereas Pt alloys behaved in a refractory manner. One could go further to suggest that the relatively high Pt/Pd in much of the Bushveld Complex is due to mobilisation of Pd from the centre to the margins of the complex, as has been suggested by Boudreau (2019) for Stillwater. In order to test this model, detailed traverses have to be sampled and analysed across all lobes of the RLS.

Another possibility is that Pd could be derived from the sedimentary floor rocks from where it was transported by metamorphic fluids into the basal portion of intrusions. Stephenson (2018) has shown that the sedimentary floor rocks of the Bushveld northern lobe tend to be relatively enriched in Pt relative to Pd, possibly reflecting selective Pd removal. As the PGE content of sediments is mostly quite low (typically < 10 ppb, Wille et al. 2007; Siebert et al. 2005), large volumes of the floor would need to be processed to affect the Pd budget of the cumulates significantly. For example, assuming that a 100-m-thick cumulate package at the base of the northern limb contains 100 ppb extra Pd over the normal Pd budget, mobilisation of 10 ppb Pd from 1000 m of sedimentary rock would be required. In conclusion, local hydrothermal Pd mobility in the Bushveld Complex is supported by empirical evidence and experimental data, but it remains unclear whether this is important on a large scale.

Crystallisation of the cumulates from parent magmas having variable Pt, Pd and Au contents, resulting from pre-emplacement magma contamination or fractionation

Platinum solubility in basalt decreases with falling fO_2 (and T) (Borisov and Palme 1997; Mungall and Brenan 2014). In the context of the Bushveld Complex, one could thus suggest that the relatively low Pt/Pd at the base of the intrusion reflects pre-emplacement contamination of the initial magma with reducing (organic) material, e.g., graphitic shale that is locally abundant in the Duitschland Formation of the Transvaal Supergroup (Yudovskaya et al. 2021 and present authors' observations on Flatreef drill cores), leading to precipitation of Pt alloys prior to, or during, final emplacement. Later magma pulses forming the overlying cumulates (including the Merensky Reef) could have undergone less contamination with the floor rocks, perhaps due to armouring of the conduits by the precipitates of the early pulses. The late pulses were thus less Pt depleted. Instead, they could have assimilated some of the Pt-rich cumulates in the staging chambers and feeder conduits. However, there is currently no direct evidence for the model, e.g., in the form of Pt-depleted fine-grained sills or dykes, or floor cumulates with high Pt/Pd.

Summary and conclusions

In the present paper, we compiled Pt, Pd and Au data on Bushveld magmas as represented by fine-grained sills in the floor of the complex and Bushveld cumulates in the western and northern limbs.

Compared to global mantle-derived magmas, the Bushveld parent magmas have unusually high Pt contents and, as a result, high Pt/Pd. After examining a number of models, we conclude that the Bushveld magmas are likely of asthenospheric derivation, with a significant SCLM component being unlikely. Also, there is no clear evidence for an unusually PGE-rich mantle, e.g., containing undissolved remnants of the late veneer. The Bushveld magmas were strongly contaminated during ascent through the continental crust, facilitated by the abnormal size and heat flux of the Bushveld event. This could have led to assimilation of Pt from Pt-rich crustal rocks, potentially containing a meteoritic component. However, no Pt-rich crustal rocks are currently known to occur in the Bushveld floor.

Bushveld cumulates show more significant variation in Pt/Pd and Au/Pt than the parent magmas, suggesting that much of the observed variation in PGE ratios occurred within the Bushveld magma chamber. Likely processes include (1) primary magmatic fractionation of sulfide melts, silicate melts and PGE alloys caused by varying partitioning of PGE, potentially locally enhanced by variation in oxidation state of magma; (2) sulfide melt percolation through semi-consolidated cumulates and associated PGE fractionation, facilitated potentially by partial melting of cumulates in response to flux of volatiles; and (3) mobilisation of some PGE (particularly Pd and potentially Au) by volatiles derived from the sedimentary floor rocks or the basal cumulates.

Declarations

Conflict of interest The authors declare no competing interests.

References

Archer GJ, Mundl A, Walker RJ, Worsham EA, Bermingham KR (2017) High-precision analysis of $^{182}W/^{184}W$ and $^{183}W/^{184}W$ by negative thermal ionization mass spectrometry: per-integration oxide corrections using measured $^{18}O/^{16}O$. Int J Mass Spectrom 414:80–86

Archer GJ, Brennecka GA, Gleißner P, Stracke A, Becker H, Kleine T (2019) Lack of late-accreted material as the origin of 182W excesses in the Archean mantle: evidence from the Pilbara Craton, Western Australia. Earth Planet Sci Lett 528:115841

Barnes SJ (1993) Partitioning of the platinum group elements and gold between silicate and sulphide magmas in the Munni Munni Complex, Western Australia. Geochim Cosmochim Acta 57(6):1277–1290

Barnes SJ, Liu W (2012) Pt and Pd mobility in hydrothermal fluids: evidence from komatiites and from thermodynamic modelling. Ore Geol Rev 44:49–58

Barnes S-J, Francis D (1995) The distribution of platinum-group elements, nickel, copper, and gold in the Muskox layered intrusion, Northwest Territories, Canada. Econ Geol 90:135–154

Barnes S-J, Maier WD (2002) Platinum-group elements and microstructures of normal Merensky Reef from Impala Platinum Mines, Bushveld Complex. J Petrol 43:103–128

Barnes S-J, Ripley EM (2016) Highly siderophile and strongly chalcophile elements in magmatic ore deposits. Rev Mineral Geochem 81(1):725–774

Barnes S-J, Zientek ML, Severson MJ (1997) Ni, Cu, Au, and platinum-group element contents of sulphides associated with intraplate magmatism: a synthesis. Can J Earth Sci 34:337–351

Barnes S-J, Picard C, Giovenazzo D, Tremblay C (1992) The composition of nickel-copper sulphide deposits and their host rocks from the Cape Smith Fold Belt, Northern Quebec. Aust J Earth Sci 39(3):335–347

Barnes S-J, Maier WD, Curl E (2010) Composition of the marginal rocks and sills of the Rustenburg Layered Suite, Bushveld Complex, South Africa: implications for the formation of the platinum-group element deposits. Econ Geol 105:1481–1511

Barnes SJ, Mungall JE, Maier WD (2015) Platinum group elements in mantle melts and mantle samples. Lithos 232:395–417

Barry TL, Davies JH, Wolstencroft M, Millar IL, Zhao Z, Jian P, Safonova I, Price M (2017) Whole-mantle convection with tectonic plates preserves long-term global patterns of upper mantle geochemistry. Sci Rep 7:1–9

Borisov A, Palme H (1997) Experimental determination of the solubility of platinum in silicate melts. Geochim Cosmochim Acta 61:4349–4357

Boudreau A (2019) Hydromagmatic processes and platinum-group element deposits in layered intrusions. Cambridge University Press, 275pp

Boudreau AE, McCallum IS (1992) Concentration of platinum-group elements by magmatic fluids in layered intrusions. Econ Geol 87(7):1830–1848

Cawthorn RG, Lee CA, Schouwstra RP, Mellowship P (2002) Relationship between PGE and PGM in the Bushveld Complex. Can Mineral 40:311–328

Campbell IH, Naldrett AJ (1979) The influence of silicate: sulfide ratios on the geochemistry of magmatic sulfides. Econ Geol 74(6):1503–1506

Chazey WJ III, Neal CR (2005) Platinum-group element constraints on source composition and magma evolution of the Kerguelen Plateau using basalts from ODP Leg 183. Geochim Cosmochim Acta 69(19):4685–4701

Chung HY, Mungall JE (2009) Physical constraints on the migration of immiscible fluids through partially molten silicates, with special reference to magmatic sulfide ores. Earth Planet Sci Lett 286:14–22

Dale CW, Kruijer TS, Burton KW (2017) Highly siderophile element and 182W evidence for a partial late veneer in the source of 3.8 Ga rocks from Isua. Greenland Earth and Planetary Science Letters 458:394–404

Day JM, Pearson DG, Hulbert LJ (2013) Highly siderophile element behaviour during flood basalt genesis and evidence for melts from intrusive chromitite formation in the Mackenzie large igneous province. Lithos 182:242–258

Day JM, Brandon AD, Walker RJ (2016) Highly siderophile elements in Earth, Mars, the Moon, and asteroids. Rev Mineral Geochem 81:161–238

Dietz RS (1963) Vredefort Ring-Bushveld Complex impact event and lunar maria. Geol. Soc. America, Spec. Paper 73: 35

Finnigan CS, Brenan JM, Mungall JE, McDonough WF (2008) Experiments and models bearing on the role of chromite as a collector of platinum group minerals by local reduction. J Petrol 49:1647–1665

Fiorentini ML, Barnes SJ, Maier WD, Heggie GJ (2011) Global variability in the PGE contents of komatiites. J Petrol 52:82–112

Fischer-Gödde M, Elfers BM, Münker C, Szilas K, Maier WD, Messling N, Morishita T, Van Kranendonk M, Smithies H (2020) Ruthenium isotope vestige of Earth's pre-late-veneer mantle preserved in Archaean rocks. Nature 579:240–244

French BM, Hargraves RB (1971) Bushveld Igneous Complex, South Africa: absence of shock-metamorphic effects in a preliminary search. J Geol 79:616–620

Godel B, Barnes SJ, Maier WD (2006) 3-D distribution of sulphide minerals in the Merensky Reef (Bushveld Complex, South Africa) and the JM Reef (Stillwater Complex, USA) and their relationship to microstructures using X-ray computed tomography. J Petrol 47:1853–1872

Grobler DF, Brits JAN, Maier WD, Crossingham A (2019) Litho- and chemostratigraphy of the Flatreef PGE deposit, northern Bushveld Complex. Miner Deposita. https://doi.org/10.1007/s00126-012-0436-1

Hamilton W (1970) Bushveld Complex–product of impacts?: Geological Society of South Africa Special Publication 1: 367–374

Hanley JJ (2005) The aqueous geochemistry of the platinum-group elements (PGE) in surficial, low-T hydrothermal and high-T magmatic-hydrothermal environments. Exploration for Platinum-Group Element Deposits 35:35–56

Harris C, Pronost JJ, Ashwal LD, Cawthorn RG (2005) Oxygen and hydrogen isotope stratigraphy of the Rustenburg Layered Suite, Bushveld Complex: constraints on crustal contamination. J Petrol 46(3):579–601

Helmy HM, Botcharnikov R, Ballhaus C, Deutsch-Zemlitskaya A, Wirth R, Schreiber A, Buhre S, Häger T (2021) Evolution of magmatic sulfide liquids: how and when base metal sulfides crystallize? Contrib Miner Petrol 176:1–15

Helz R (1987) Evidence for melt extraction from the sills and dikes associated with the Stillwater Complex. Montana Geol Soc America Abstracts Program 19:699

Holwell DA, Jones A, Smith JW, Boyce AJ (2013) New mineralogical and isotopic constraints on Main Zone-hosted PGE mineralisation at Moorddrift, northern Bushveld Complex. Miner Deposita 48:675–686

Holwell DA, Adeyemi Z, Ward LA, Smith DJ, Graham SD, McDonald I, Smith JW (2017) Low temperature alteration of magmatic Ni-Cu-PGE sulfides as a source for hydrothermal Ni and PGE ores: a quantitative approach using automated mineralogy. Ore Geol Rev 91:718–740

Horan MF, Walker RJ, Morgan JW, Grossman JN, Rubin AE (2003) Highly siderophile elements in chondrites. Chem Geol 196:27–42

Hutchinson D, McDonald I (2008) Laser ablation ICP-MS study of platinum-group elements in sulphides from the Platreef at Turfspruit, northern limb of the Bushveld Complex, South Africa. Miner Deposita 43:695–711

Ihlenfeld C, Keays RR (2011) Crustal contamination and PGE mineralization in the Platreef, Bushveld Complex, South Africa: evidence for multiple contamination events and transport of magmatic sulfides. Miner Deposita 46:813–832

Kamo SL, Reimold WU, Krogh TE, Colliston WP (1996) A 2.023 Ga age for the Vredefort impact event and a first report of shock metamorphosed zircons in pseudotachylitic breccias and granophyre. Earth Planet Sci Lett 144:369–387

Kennedy B (2018) Unconventional olivine-rich cumulates, magma dynamics and development of platinum-group element mineralisation in the Main Zone of the northern Bushveld Complex (Doctoral dissertation, Cardiff University), 457pp

Kinnaird JA (2005) Geochemical evidence for multiphase emplacement in the southern Platreef. Appl Earth Sci 114(4):225–242

Kinnaird JA, McDonald I (2018) The northern limb of the Bushveld Complex: a new economic frontier. Soc Econ Geol Spec Publ 21:157–176

Kinnaird JA, Hutchinson D, Schurmann L, Nex PAM, de Lange R (2005) Petrology and mineralization of the southern Platreef: northern limb of the Bushveld Complex, South Africa. Miner Deposita 40:576–597

Kinnaird JA, Yudovskaya M, McCreesh M, Huthmann F, Botha TJ (2017) The Waterberg platinum group element deposit: atypical mineralization in mafic-ultramafic rocks of the Bushveld Complex, South Africa. Econ Geol 112:1367–1394

Kleine T, Münker C, Mezger K, Palme H (2002) Rapid accretion and early core formation on asteroids and the terrestrial planets from Hf–W chronometry. Nature 418:952–955

Kruger FJ, Marsh JS (1982) Significance of 87Sr/86Sr ratios in the Merensky cyclic unit of the Bushveld Complex. Nature 298(5869):53–55

Kruijer TS, Kleine T (2018) No 182W excess in the Ontong Java Plateau source. Chem Geol 485:24–31

Leeb-Du Toit A (1986) The Impala platinum mines. In: mineral deposits of Southern Africa. pp 1091–1106

Li C, Ripley EM, Sarkar A, Shin D, Maier WD (2005) Origin of phlogopite-orthopyroxene inclusions in chromites from the Merensky Reef of the Bushveld Complex, South Africa. Contrib Mineral Petrol 150(1):119–130

Li J, Wang XC, Ren ZY, Xu JF, He B, Xu YG (2014) Chemical heterogeneity of the Emeishan mantle plume: evidence from highly siderophile element abundances in picrites. J Asian Earth Sci 79:191–205

Liu J, Touboul M, Ishikawa A, Walker RJ, Pearson GD (2016) Widespread tungsten isotope anomalies and W mobility in crustal and mantle rocks of the Eoarchean Saglek Block, northern Labrador, Canada: implications for early Earth processes and W recycling. Earth Planet Sci Lett 448:13–23

Maier WD, Barnes S-J (2004) Pt/Pd and Pd/Ir ratios in mantle-derived magmas: a possible role for mantle metasomatism. S Afr J Geol 107:333–340

Maier WD, Barnes S-J (2008) Platinum-group elements in the UG1 and UG2 chromitites and the Bastard reef at Impala platinum mine, western Bushveld Complex. S Afr J Geol 111:159–176

Maier WD, Barnes S-J (2010) The petrogenesis of PGE reefs in the upper Main Zone of the northern lobe of the Bushveld Complex on the farm Moorddrift, South Africa. Econ Geol 105:841–854

Maier WD, Arndt NT, Curl EA (2000) Progressive crustal contamination of the Bushveld Complex: evidence from Nd isotopic analyses of the cumulate rocks. Contrib Mineral Petrol 140(3):316–327

Maier WD, de Klerk L, Blaine J, Manyeruke T, Barnes S-J, Stevens MVA, Mavrogenes JA (2008) Petrogenesis of contact-style PGE mineralization in the northern lobe of the Bushveld Complex: comparison of data from the farms Rooipoort, Townlands, Drenthe and Nonnenwerth. Miner Deposita 43:255–280

Maier WD, Barnes SJ, Campbell IH, Fiorentini ML, Peltonen P, Barnes S-J, Smithies RH (2009) Mantle magmas reveal progressive mixing of meteoritic veneer into the early Earth's deep mantle. Nature 460:620–623

Maier WD, Peltonen P, McDonald I, Barnes SJ, Barnes S-J, Hatton C, Viljoen F (2012) The concentration of platinum-group elements and gold in southern African and Karelian kimberlite-hosted mantle xenoliths: implications for the noble metal content of the Earth's mantle. Chem Geol 302–303:119–135

Maier WD, Barnes S-J, Groves DI (2013) The Bushveld Complex, South Africa: formation of platinum-palladium, chrome and vanadium-rich layers via hydrodynamic sorting of a mobilized cumulate slurry in a large, relatively slowly cooling, subsiding magma chamber. Miner Deposita 48:1–56

Maier WD, Barnes S-J, Karykowski BT (2016) A chilled margin of komatiite and Mg-rich basaltic andesite in the western Bushveld Complex, South Africa. Contributions to Mineralogy and Petrology, DOI https://doi.org/10.1007/s00410-016-1257-5.

Maier WD, Prevec SA, Scoates JS, Wall CJ, Barnes S-J, Gomwe T (2017) The Uitkomst intrusion and Nkomati Ni-Cu-Cr-PGE deposit, South Africa: trace element geochemistry, Nd isotopes, and high-precision geochronology. Miner Deposita. https://doi.org/10.1007/s00126-017-0716-x

Maier WD, Abernethy KEL, Grobler DF, Moorhead G (2021) Formation of the Flatreef deposit, northern Bushveld, by hydrodynamic

and hydromagmatic processes. Miner Deposita. https://doi.org/10.1007/s00126-020-00987-5
Maier WD, Barnes SJ, Godel BM, Grobler D, Smith WD (2022) The TMT006 bonanza PGE intersections of the Flatreef, Bushveld northern limb (submitted)
Manyeruke TD (2007) Geochemical variation of the Platreef in the northern limb of the Bushveld Complex: implications for the origin of the PGE mineralization. University of Pretoria
Manyeruke T, Maier WD, Barnes S-J (2005) Major and trace element geochemistry of the Platreef on the farm Townlands, northern Bushveld Complex. S Afr J Geol 108:379–396
McCandless TE, Ruiz J (1991) Osmium isotopes and crustal sources for platinum-group mineralization in the Bushveld Complex, South Africa. Geology 19:1225–1228
McDonald I, Ohnenstetter D, Rowe JP, Tredoux M, Pattrick RAD, Vaughan DJ (1999) Platinum precipitation in the Waterberg deposit, Naboomspruit, South Africa. S Afr J Geol 102:184–191
McDonald I, Harmer RJ, Holwell DA, Hughes HS, Boyce AJ (2017) Cu-Ni-PGE mineralisation at the Aurora Project and potential for a new PGE province in the Northern Bushveld Main Zone. Ore Geol Rev 80:1135–1159
McLaren CH, De Villiers JP (1982) The platinum-group chemistry and mineralogy of the UG-2 chromitite layer of the Bushveld Complex. Econ Geol 77:1348–1366
Mei Q-F, Yang J-H, Wang Y-F, Wang H, Peng HP (2020) Tungsten isotopic constraints on homogenization of the Archean silicate Earth: implications for the transition of tectonic regimes. Geochim Cosmochim Acta 278:51–64
Mundl A, Touboul M, Jackson MG, Day JMD, Kurz MD, Lekic V, Helz RT, Walker RJ (2017) Tungsten-182 heterogeneity in modern ocean island basalts. Science 356:66
Mundl A, Walker RJ, Reimink JR, Runick RL, Gaschnig RM (2018) Tungsten-182 in the upper continental crust: evidence from glacial diamictites. Chem Geol 494:144–152
Mundl-Petermeier A, Walker RJ, Jackson MG, Blichert-Toft J, Kurz MD (2019) Temporal evolution of primordial tungsten-182 and 3He/4He signatures in the Iceland mantle plume. Chem Geol 525:245–259
Mundl-Petermeier A, Walker RJ, Fischer RA, Lekic V, Jackson MG, Kurz MD (2020) Anomalous 182W in high 3He/4He ocean island basalts: fingerprints of Earth's core? Geochim Cosmochim Acta 271:194–211
Mungall JE, Su S (2005) Interfacial tension between magmatic sulfide and silicate liquids: constraints on kinetics of sulfide liquation and sulfide migration through silicate rocks. Earth Planet Sci Lett 234:135–149
Mungall JE, Brenan JM (2014) Partitioning of platinum-group elements and Au between sulfide liquid and basalt and the origins of mantle-crust fractionation of the chalcophile elements. Geochim Cosmochim Acta 125:265–289
Nakanishi N, Giuliani A, Carlson RW, Horan MF, Woodhead J, Pearson DG, Walker RJ (2021) Tungsten-182 evidence for an ancient kimberlite source. Proc Natl Acad Sci 118:e2020680118
Naldrett AJ (2004) Magmatic sulfide deposits: geology, geochemistry and exploration. Springer Science & Business Media
Naldrett AJ, Lehmann J (1988) Spinel non-stoichiometry as the explanation for Ni-, Cu- and PGE-enriched sulphides in chromitites. In Prichard HM and Potts PJ (eds), Geo-platinum 87. Springer Science & Business Media, 93–109
Naldrett AJ, Wilson A, Kinnaird J, Chunnett G (2009) PGE tenor and metal ratios within and below the Merensky Reef, Bushveld Complex: implications for its genesis. J Petrol 50:625–659
Naldrett AJ, Wilson A, Kinnaird J, Yudovskaya M, Chunnett G (2012) The origin of chromitites and related PGE mineralization in the Bushveld Complex: new mineralogical and petrological constraints. Miner Deposita 47:209–232
Nwaila GT, Frimmel HE (2019) Highly siderophile elements in Archaean and Palaeoproterozoic marine shales of the Kaapvaal Craton, South Africa. Mineral Petrol 113:307–327
Peregoedova A, Barnes S-J, Baker DR (2004) The formation of Pt–Ir alloys and Cu–Pd-rich sulfide melts by partial desulfurization of Fe–Ni–Cu sulfides: results of experiments and implications for natural systems. Chem Geol 208:247–264
Peregoedova A, Barnes S-J, Baker DR (2006) An experimental study of mass transfer of platinum-group elements, gold, nickel and copper in sulfur-dominated vapor at magmatic temperatures. Chem Geol 235:59–75
Peters BJ, Mundl-Petermeier A, Horan MF, Carlson RW, Walker RJ (2019) Chemical separation of tungsten and other trace elements for TIMS isotope ratio measurements using organic acids. Geostand Geoanal Res 43:245–259
Peters BJ, Mundl-Petermeier A, Carlson RW, Walker RJ, Day JMD (2021) Combined lithophile-siderophile isotopic constraints on Hadean processes preserved in ocean island basalt sources. Geochemistry, Geophysics, Geosystems 22: e2020GC009479
Puchtel IS, Blichert-Toft J, Touboul M, Horan MF, Walker RJ (2016a) The coupled 182W–142Nd record of early terrestrial mantle differentiation. Geochem Geophys Geosyst 17:2168–2193
Puchtel IS, Touboul M, Blichert-Toft J, Walker RJ, Brandon AD, Nicklas RW, Kulikov VS, Samsonov AV (2016b) Lithophile and siderophile element systematics of Earth's mantle at the Archean-Proterozoic boundary: evidence from 2.4 Ga komatiites. Geochim Cosmochim Acta 180:227–255
Puchtel IS, Blichert-Toft J, Touboul M, Walker RJ (2018) 182W and HSE constraints from 2.7 Ga komatiites on the heterogeneous nature of the Archean mantle. Geochim Cosmochim Acta 228:1–26
Puchtel IS, Mundl-Petermeier A, Horan M, Hanski EJ, Blichert-Toft J, Walker RJ (2020) Ultra-depleted 2.05 Ga komatiites of Finnish Lapland: products of grainy late accretion or core-mantle interaction? Chemical Geology 554:119801
Reimink JR, Chacko T, Carlson RW, Shirey SB, Liu J, Stern RA, Bauer AM, Pearson DG, Heaman LM (2018) Petrogenesis and tectonics of the Acasta Gneiss Complex derived from integrated petrology and 142Nd and 182W extinct nuclide-geochemistry. Earth Planet Sci Lett 494:12–22
Reimink JR, Mundl-Petermeier A, Carlson RW, Shirey SB, Walker RJ, Pearson DG (2020) Tungsten isotope composition of archean crustal reservoirs and implications for terrestrial μ182W evolution. Geochem Geophys Geosyst 21:e2020GC009155
Rhodes RC (1975) New evidence for impact origin of the Bushveld Complex, South Africa. Geology 3:554–549
Richardson SH, Shirey SB (2008) Continental mantle signature of Bushveld magmas and coeval diamonds. Nature 453(7197):910–913
Rizo H, Walker RJ, Carlson RW, Touboul M, Horan MF, Puchtel IS, Boyet M, Rosing MT (2016) Early Earth differentiation investigated through 142Nd, 182W, and highly siderophile element abundances in samples from Isua, Greenland. Geochim Cosmochim Acta 175:319–336
Rizo H, Andrault D, Bennett NR, Humayun M, Brandon A, Vlastelic I, Moine B, Poirier A, Bouhifd MA, Murphy DT (2019) 182W evidence for core-mantle interaction in the source of mantle plumes. Geochemical Perspectives Letters 11:6–11
Sharpe MR (1981) The chronology of magma influxes to the eastern compartment of the Bushveld Complex as exemplified by its marginal border groups. J Geol Soc 138(3):307–326
Sharpe MR, Hulbert LJ (1985) Ultramafic sills beneath the eastern Bushveld Complex; mobilized suspensions of early lower zone cumulates in a parental magma with boninitic affinities. Econ Geol 80:849–871
Siebert C, Kramers JD, Meisel T, Morel P, Nägler TF (2005) PGE, Re-Os, and Mo isotope systematics in Archean and early

Proterozoic sedimentary systems as proxies for redox conditions of the early Earth. Geochim Cosmochim Acta 69:1787–1801
Smith WD, Maier WD (2021) The geotectonic setting, age and mineral deposit inventory of global layered intrusion. Earth-Sci Rev 220:103736
Smith WD, Maier WD, Barnes SJ, Moorhead G, Reid D, Karykowski B (2020) Element mapping the Merensky Reef of the Bushveld Complex. Geosci Front. https://doi.org/10.1016/j.gsf.2020.11.001
Stephenson H (2018) The Platreef magma event at the world-class Turfspruit Ni-Cu-PGE deposit: implications for mineralisation processes and the Bushveld Complex stratigraphy (Doctoral dissertation, Cardiff University), 454 pp
Stevenson D (1981) Models of the Earth's core. Science 214:611–618
Sullivan NA, Zajacz Z, Brenan JM, Tsay A (2021) The solubility of platinum in magmatic brines: insights into the mobility of PGE in ore-forming environments. Geochim Cosmochim Acta 316:253–327
Tappe S, Budde G, Stracke A, Wilson A, Kleine T (2020) The tungsten-182 record of kimberlites above the African superplume: exploring links to the core-mantle boundary. Earth Planet Sci Lett 547:116473
Touboul M, Puchtel IS, Walker RJ (2012) 182W Evidence for long-term preservation of early mantle differentiation products. Science 335:1065
Touboul M, Liu J, O'Neil J, Puchtel IS, Walker RJ (2014) New insights into the Hadean mantle revealed by 182W and highly siderophile element abundances of supracrustal rocks from the Nuvvuagittuq Greenstone Belt, Quebec, Canada. Chem Geol 383:63–75
Tusch J, Sprung P, Van de Löcht J, Hoffmann JE, Boyd AJ, Rosing MT, Münker C (2019) Uniform 182W isotope compositions in Eoarchean rocks from the Isua region, SW Greenland: the role of early silicate differentiation and missing late veneer. Geochim Cosmochim Acta 257:284–310
Tusch J, Münker C, Hasenstab E, Jansen M, Marien CS, Kurzweil F, Van Krankendonk MJ, Smithies H, Maier WD, Garbe-Schönberg D (2021a) Convective isolation of Hadean mantle reservoirs through Archean time. Proc Natl Acad Sci 118:e2012626118
Tusch J, Hoffmann E, Hasenstab E, Münker C (2021b) Long-term preservation of Hadean protocrust in Earth's mantle. Earth Space Sci Open Archive 39:https://doi.org/10.1002/essoar.10507464.1
Vockenhuber C, Oberli F, Bichler M, Ahmad I, Quitté G, Meier M, Halliday AN, Lee DC, Kutschera W, Steier P, Gehrke RJ (2004) New half-life measurement of H f 182: improved chronometer for the early solar system. Phys Rev Lett 93(17):172501
Von Gruenewaldt G, Merkle RKW (1995) Platinum group element proportions in chromitites of the Bushveld complex: implications for fractionation and magma mixing models. J Afr Earth Sc 21:615–632
Walker RJ (2009) Highly siderophile elements in the Earth, Moon and Mars: update and implications for planetary accretion and differentiation. Geochemistry 69:101–125
Walker RJ (2016) Siderophile elements in tracing planetary formation and evolution. Geochemical perspectives 5: 145pp
Willbold M, Elliott T, Moorbath TS (2011) The tungsten isotopic composition of the Earth's mantle before the terminal bombardment. Nature 477:195–198
Willbold M, Mojzsis SJ, Chen H-W, Elliott T (2015) Tungsten isotope composition of the Acasta Gneiss Complex. Earth Planet Sci Lett 419:168–177
Wille M, Kramers JD, Nägler TF, Beukes NJ, Schröder S, Meisel T, Lacassie JP, Voegelin AR (2007) Evidence for a gradual rise of oxygen between 2.6 and 2.5 Ga from Mo isotopes and Re-PGE signatures in shales. Geochim Cosmochim Acta 71:2417–2435
Wulf AV, Palme H, Jochum KP (1995) Fractionation of volatile elements in the early solar system: evidence from heating experiments on primitive meteorites. Planet Space Sci 4
Wilson AH (2001) Compositional and lithological controls on the PGE-bearing sulphide zones in the Selukwe Subchamber, Great Dyke: a combined equilibrium–Rayleigh fractionation model. J Petrol 42(10):1845–1867
Yao Z, Mungall JE, Jenkins MC (2021) The Rustenburg Layered Suite formed as a stack of mush with transient magma chambers. Nat Commun 12:1–13
Yudovskaya MA, Costin G, Sluzhenikin SF, Kinnaird JA, Ueckermann H, Abramova VD, Grobler DF (2021) Hybrid norite and the fate of argillaceous to anhydritic shales assimilated by Bushveld melts. Mineral Deposita 56(1):73–90